C.P. No. 1013

C.P. No. 1013

MINISTRY OF TECHNOLOGY

AERONAUTICAL RESEARCH COUNCIL

CURRENT PAPERS

The Influence of Density Gradients on the Effectiveness of Film Cooling

By

B. R. Pai and J H. Whitelaw

LONDON. HER MAJESTY'S STATIONERY OFFICE

1968

Price 6s. 6d. net

C.P. No.1013*

December, 1967

The Influence of Density Gradients on the Effectiveness of Film Cooling

- By -
B. R. Pai and J. H. Whitelaw,
Department of Mechanical Engineering,
Imperial College of Science and Technology

SUMMARY

New measurements of the impervious-wall effectiveness are presented in the range of the velocity ratio

$$0.3 \leq \bar{u}_C/u_G \leq 3.1 \quad .$$

These measurements were carried out using hydrogen, air, argon and Arcton 12 as the injected gas: the resulting range of density ratios was

$$0.07 \leq \rho_C/\rho_G \leq 4.17 \quad .$$

The measurements demonstrate, quantitatively, that an increase in the density ratio leads to an increase in effectiveness for the same velocity ratio.

The prediction method proposed by S. V. Patankar and D. B. Spalding has been tested against the present measurements and shown to be a convenient method in the region downstream of the immediate vicinity of the slot exit. The predictions are reasonable but it is concluded that further experimental work is necessary to establish the appropriate distribution of the effective Schmidt (or Prandtl) number.

CONTENTS

---

*Replaces Imperial College Ref. EHT/TN/8 - A.R.C.29 928.

1. Introduction

The purpose of this paper is to report the progress in an investigation of the influence of density gradients on the adiabatic-wall effectiveness of film cooling in steady, two-dimensional flow. The research program has as its objective, the provision of a procedure for predicting the effectiveness in the presence of density and pressure gradients but the present paper is concerned only with density gradients. The influence of density gradients is of considerable importance in gas turbine practice when film cooling is employed with large temperature gradients.

The provision of a satisfactory prediction procedure implies that it must be tested against reliable experimental data. For present purposes, this implies that it should be tested against experimental data which include appreciable density gradients but which exclude other variables whose influence is not well known. Unfortunately, little experimental information of this type has been reported in the literature: only reference 1 contains measurements with a wider range of density gradients. References 2, 3 and 4 also contains relevant information. The shortage of experimental information led the present authors to undertake an experimental program and much of the present paper is concerned with the description of the experimental method and the presentation of the results.

The measurements reported were carried out by injecting a foreign gas tangentially into a free-stream of air: hydrogen, air, argon and Arcton 12 were each employed as the foreign gas giving density ratios in the range $0.07 \leq \rho_G/\rho_C \leq 4.1$. Foreign gas injection was employed because it permits large density gradients to be achieved at room temperature conditions. The impervious-wall effectiveness was measured rather than the adiabatic-wall effectiveness because this implied that a temperature gradient was not required to be superimposed on the existing density gradient: the mass transfer measurements are, of course, analagous to heat transfer measurements and can readily be used to represent the effects of density gradients which arise as a result of temperature gradients.

The prediction procedure is based on the work of S. V. Patankar and D. B. Spalding (5): this paper describes a numerical procedure for solving the steady, two-dimensional boundary-layer equations and is applicable to film cooling situations in the region downstream of the slot where separated flow and pressure gradients normal to the flow are absent. The region close to the slot exit cannot exactly be described by the boundary-layer equations but it is likely that they can be employed with reasonable precision for slot geometries which are two-dimensional and which have a relatively thin upper lip. Work is in progress to test this possibility*, but the present paper will be concerned with the prediction procedure only in the region downstream of the slot. This further limits the experimental information which can be used for testing the procedure since profiles of velocity and temperature (or mass fraction) must be available in order to begin the integration: the measurements reported in this paper include profiles of velocity and mass fraction at suitable locations downstream of the slot exit.

2. Apparatus and experimental procedure

It is convenient to describe the apparatus in four separate sections concerned with, respectively, the wind tunnel, the secondary gas circuit, the measurement of impervious-wall effectiveness and the overall experimental procedure. The general layout of the apparatus is shown in figure 1.

---

* work is also underway to solve the Navier-Stokes equations which are applicable in the region close to the slot.

2.1 Wind tunnel

The suction wind tunnel shown in figure 1 had a contraction with an area ratio of 19.2 . The plenum chamber upstream of the contraction contained a $\frac{1}{2}$" x $\frac{1}{2}$" x 2" honeycomb which was followed by two 28 swg x 20 mesh copper screens, 14 inches apart. The working section was 6 in x 5 in x 6 ft long and was constructed from Dural and Perspex: the base plate was made of Dural. The centrifugal fan was capable of producing velocities of up to 150 ft/s in the working section: the freestream turbulence level was approximately 0.35% at 60 ft/s.

The base plate of the wind tunnel contained a number of static pressure holes which were designed in accordance with the recommendations of reference 6 and which also served as sampling holes, as described in section 2.3 . One side wall of the wind tunnel also contained a number of static pressure holes since, in the region close to the slot, the static pressure measured on the tunnel base plate did not apply to the free-stream.

The total head pressures were measured using flattened probes which were carried on a micrometer controlled traverse which was operated from the top of the working section. Where necessary, a rake of probes was used. The probe dimensions were of the order of: outside - 0.009 in x 0.055 in; inside - 0.004 in x 0.045 in.

2.2 Secondary circuit

The secondary circuit was identical for the injection of hydrogen, argon and Arcton 12. In these cases the gas was taken from cylinders passed through a manifold and into a straight length of 3 inch diameter pipe which contained an orifice plate designed in accordance with BS 1052, 1966. The gas then passed into a plenum chamber before passing through the injection slot. The flow rate of gas was controlled by a throttle valve located on the downstream side of the gas manifold.

In the particular case where air was used as the secondary gas, a small blower was located upstream of the straight length of 3 inch diameter pipe. The flow rate of air was controlled by a slide plate on the suction side of the blower.

For all measurements, the slot configuration was the same: the essential dimensions are given in figure 2.

2.3 The measurement of impervious-wall effectiveness

The impervious-wall effectiveness was obtained by measuring the mass concentration of secondary gas at the base plate of the wind tunnel and in the free-stream: the impervious-wall effectiveness is then defined as:

$$\eta_I \equiv \frac{c_S - c_G}{c_C - c_G}$$

where c is the mass fraction of secondary gas and the subscripts S, C and G refer to the wall, the slot and the free-stream respectively. The measurements of the mass fraction can be conveniently described in two parts, the first concerned with obtaining the sample and the second with the analysis of the sample. The technique employed has been described in detail in reference 7 and, consequently, the present description will be brief.

The gas samples were obtained using sample bottles of the type shown on figure 3. A rotary vacuum pump was used to draw samples through the static pressure holes in the base plate of the wind tunnel: the samples were collected over high vacuum oil. The rate of sampling was sufficiently low as to ensure

that the resulting concentration was not a function of the sampling rate.

The mass fraction of the samples were determined with the aid of a Shandon KG2 Gas Chromatograph: a 2 metre, molecular sieve column was employed together with a thermal conductivity cell. The samples were drawn from the sample bottles using a 1 ml gas tight hypodermic syringe and were injected into the chromatograph: the output from the thermal conductivity cell was traced by a recorder and "peak heights" were used to indicate the various concentrations. The instrument was calibrated for each gas used: the calibration was carried out before and after the effectiveness measurements with each gas.

For the air into air measurements, the secondary air contained a tracer of helium gas which was added at the pressure side of the secondary blower. In this case, the effectiveness was determined by measuring the mass concentrations of helium in air.

Profiles of mass concentration were measured in a similar manner to that of impervious-wall effectiveness. The rakes used to measure the total head pressures were used in the same manner as the base plate static pressure holes: the sample bottles were connected to the total head pressure probes rather than to the static pressure holes.

2.4 Experimental procedure

The simplest way in which to describe the experimental procedure is to give a sequential description of the measurements of secondary mass flow rate, velocity profiles, concentration profiles and impervious-wall effectiveness for a particular secondary gas and for one value of u_C/u_G. The sequence is slightly different for the case of air (plus helium tracer) into air than for the three other gases and, since the method for air into air is adequately described in reference 8, the following description applies to the injection of hydrogen, argon or Arcton 12.

The mainstream and seondary stream velocities were set to the required nominal value; the former by measuring the total head and static pressure and the second with the aid of the orifice plate reading. The total head pressure, static pressure distribution and orifice pressure drop were recorded. Gas samples were then drawn through the static pressure holes in the tunnel base plate and collected in the sample bottles for subsequent analysis. In cases where concentration and velocity profiles were measured, a rake of probes was fixed in the required location and the total head pressures recorded; an arrangement of quick acting valves was then used to connect the probes to the sampling bottles and samples were drawn in the usual way.

For the case of hydrogen injection, the seondary line was flushed with nitrogen before and after each experimental run.

3. Presentation and discussion of experimental results

The results of the present experimental investigation are given in Tables 1, 2, 3 and 4 for hydrogen, air, argon and Arcton 12 injection, respectively: some of the results are also shown diagrammatically on figures 4 and 5.

It may be seen from figure 4 that the scatter of effectiveness measurements about a smooth curve is small, around 2% of unity: this compares with a value of 3% of unity which is the precision calculated by adding up possible source of error such as are incurred by the calibration of the chromatograph, and the concentration measurement. Reproducibility tests have

also been carried out, i.e. the velocity ratio for a particular injected gas was reset and the effectiveness measurements repeated; the reproducibility was of the order of 3% of unity. The errors incurred in the measurement of $\bar{u}_C/u_G$ and x/y_C were at all times of less significance than those of effectiveness.

Figure 4 also indicates that the tendency for the effectiveness to increase with $\bar{u}_C/u_G$, to reach a maximum close to a value of $\bar{u}_C/u_G$ of unity and to fall again to a constant, and lower, value is not present for the measurements with Arcton 12. This tendency had previously been noted for air into air measurements in references 7, 8, 9 and 10. The figure implies that for high density ratios there is no significant advantage in employing a velocity ratio of greater than approximately unity; for density ratios around unity it can be disadvantageous; but for low density ratios it is highly advantageous.

The influence of density is shown clearly by figure 5 from which it is obvious that the denser the secondary gas, the higher will be the effectiveness for a prescribed velocity ratio. It is of interest to note that a typical gas-turbine density ratio is of the order of 3 and that this implies an optimum velocity ratio of approximately unity.

In references 9 and 10 it was demonstrated that the influence of the ratio of slot lip thickness to slot height, t/y_C is considerable: the effectiveness was shown to decrease substantially as t/y_C was increased. The present measurements were carried out with a tapered slot lip so that an absolute value of t is difficult to define. Figure 6 compares the air injection measurement of reference 9 ($t/y_C = 0.124$) with the present results: it may be seen that the present effectiveness values are lower in all cases. The present slot (figure 2) had a slot lip of 0.06 inch thickness which was tapered to approximately 0.01 inch over a distance of 0.5 inches: the results shown in figure 6, together with these contained in reference 9, suggest that the effective value of t/y_C for the present slot configuration is of the order of 0.3.

4. The prediction procedure

The computational method reported in reference 5 can be applied to the solution of any parabolic differential equation: this includes the boundary-layer equations, which are applicable in the region downstream of a film cooling slot but not in the immediate vicinity of the slot. The details of the procedure are described in detail in reference 5 and need not be repeated here. The modifications which have been made to this procedure for the present application are described in section 4.1 and the comparisons between the resulting procedure and experimental data are described in section 4.2.

4.1 The amended procedure

For the film cooling application, the equations to be solved are the two-dimensional momentum equation

$$\left.\frac{\partial u}{\partial x}\right|_{\psi} = \left.\frac{\partial \tau}{\partial \psi}\right|_{x} - \frac{1}{\rho u}\frac{dp}{dx}$$

and the species equation

$$\left.\frac{\partial c}{dx}\right|_{\psi} = -\left.\frac{\partial J}{\partial \psi}\right|_{x}$$

where $d\psi \equiv \rho u dy$.

The boundary conditions are:

$$\psi = 0, \quad u = J = 0$$

$$\psi = \psi_G, \quad u = u_G = \text{constant}.$$

The two conservation equations are linked by the expression

$$\rho = \frac{p}{RT} \quad \frac{M_C \cdot M_G}{(M_G \cdot c + (1 - c)M_C)}$$

and it is assumed that the mixing process is isothermal.

The above conditions have been imposed within the framework of the computer program reported in reference 5. Thus, it remains only to specify

$$\tau = \tau(\psi)$$

and

$$J = J(\psi) \ .$$

The shear stress distribution recommended for wall flows was

$$\tau = \rho \ell^2 \left|\frac{\partial u}{\partial y}\right| \frac{\partial u}{\partial y}$$

$$\text{i.e.} \quad \mu_{eff} = \rho \ell^2 \left|\frac{\partial u}{\partial y}\right|$$

$$\text{where} \quad \ell = Ky, \qquad 0 < y < \frac{\lambda y_G}{K}$$

$$\ell = \lambda y_G, \qquad \frac{\lambda y_G}{K} < y < y_G$$

where λ and K are constants and y_G is the boundary layer thickness.

The mass flux distribution is given by the equation

$$J = - \left[\frac{\rho \ell^2 |\partial u/\partial y|}{\sigma_{eff}}\right] \frac{\partial c}{\partial y}$$

where σ_{eff} is the effective Schmidt number and is constant.

Some of the predictions presented in section 4.2 have been obtained using the recommendations of the previous paragraph but it can be anticipated that, under certain circumstances, these recommendations may not be entirely satisfactory. Specifically, in cases where the velocity gradient becomes zero, the above flux laws will lead to zero flux: this is unlikely to occur in practice. Thus, in jet like flows (i.e. with a velocity maximum) and in wake like flows downstream of a slot of finite lip thickness (usually leading to a velocity profile with a region of constant velocity) both the momentum and mass fluxes will be set to zero over a finite portion of the boundary layer. To overcome these

possible disadvantages, the modified program includes provision for "bridging" the effective viscosity profile for either or both of the shear stress and mass flux calculations. This bridging procedure is best understood with the aid of a diagram. Figure 7 shows, with a full line the eddy viscosity profiles which result from the indicated velocity profiles: the dotted line indicates the bridging procedure which can be used in the program.

4.2 Comparison of experiment and predictions

In order to test the validity of a prediction procedure, it is necessary to know the boundary conditions and desirable to be able to compare predicted and measured profiles, in addition to wall values of conserved properties. For present purposes, the wall and free-stream boundary conditions are restricted to

$$y = y_G, \quad du_G/dx = da_G/dx = 0$$

$$y = 0, \quad u = v = 0.$$

The profiles of velocity and species (or enthalpy) must also be known at the initial station, i.e. $x/y_G = 20$. As will be seen in the following sub-sections, profiles are seldom reported in the literature and, consequently, most of the comparisons are with the authors' own experimental data.

In addition to the boundary conditions, distributions of effective viscosity and effective Schmidt (or Prandt) number must be known. In accordance with the recommendation of reference 5, the mixing length hypothesis is used to obtain the distribution of eddy viscosity with values of K and λ of 0.435 and 0.09 respectively: it will be seen that these values lead to reasonable predictions of the velocity profile. The specification of the effective Schmidt or Prandtl number is more difficult: in this case, there is little direct experimental evidence upon which to make a judgement. In the absence of such information, it has been the practice to assume a constant value for the Schmidt or Prandtl number but, as will be shown, this is not entirely satisfactory.

For flows with a velocity maximum, the "bridging" procedure described in section 4.1 had been applied to the distribution of mass-diffusivity only; the effective viscosity used in the valuations of velocity has been left unaltered. Tests showed that there was a negligible difference in the velocity profile with and without the "bridging" of the effective viscosity.

In order to economise on computer time, comparisons have been restricted to four blowing rates for each density ratio. It should be mentioned, however, that for the grid intervals and step length employed for these calculations (12 grid intervals and a step length such that the quantity of fluid in the boundary layer increases by 2.5% on each step), the calculation time for each value of the velocity ratio was of the order of $\frac{1}{2}$ minute for 150 integrations.

4.2-1 Comparison of experimental and predicted profiles

Figures 8a and 8b show the predicted and measured development of velocity and concentration profiles for four values of u_G/u_∞ and for a density ratio of unity: the lines represent the predicted profiles and the points represent measurements. It is evident that the velocity profiles are well predicted, the maximum deviation being of the order of 4% of the free-stream velocity.

The concentration profiles have been normalised with the wall value but even so, the profiles obtained with a constant value of Schmidt number (i.e. unity) and shown by dotted lines, do not compare well with the measured values. The concentration profiles obtained with a linear variation of effective Schmidt number (from 1.75 at the wall to 0.5 in the free-stream), and shown by full lines show better agreement with experiment.

It may be concluded from these comparisons, which are representative of many more, that the mixing length assumption is satisfactory for present purposes but that the assumption of a constant effective Schmidt number is adequate. The comparisons indicate that an effective Schmidt number distribution is required which implies an affective Schmidt number in excess of unity close to the wall and falling to 0.5 in the free stream. Further work is necessary to determine the correct form of this distribution and to the suggestion that an effective Schmidt number in excess of unity may be required close to the wall. It should, however, be noted that J. C. Rotta (12) has previously suggested that the effective Prandtl number may be in excess of unity close to the wall. The value of 0.5 for the outer edge is not surprising since it is generally accepted as being applicable to free flows.

4.2-2 Comparison of experimental and predicted values of effectiveness

Figure 9 shows measured and predicted values of the impervious wall effectiveness for a range of values of $\bar{u}_G/u_G$ and ρ_G/ρ_G. As was the case with figure 8, data have been selected to demonstrate the advantages and limitations of the prediction method. The measured points are shown as black circles; the predictions, using a constant effective Schmidt number as broken lines; and the predictions, using the linear effective Schmidt number distribution, as full lines. It may be seen that, for air, argon and Arcton 12 injection, the linear Schmidt number distribution generally leads to better predictions. The predictions for hydrogen injection are better for the case of a constant Schmidt number but, in these cases, the slot Reynolds number is low and suggests that the influence of the laminar Schmidt number may be appreciable. (The present prediction method does not take account of laminar flows although it can readily be modified to do so). Further work is necessary to confirm the suggestion that the flow regime, in the case of hydrogen injection, is laminar.

Figures 9a to d indicate predictions for constant effective Schmidt numbers of 0.5 and 1.0. The value of 0.5 was chosen to allow a comparison with the results of E. H. Cole, D. B. Spalding and J. L. Stollery (11). In this reference, the present prediction method was employed with a constant effective Schmidt number of 0.5 and with an assumed and simplified flow in the region immediately downstream of the slot: thus the integration was begun at the slot exit. The comparisons shown on figures 9a to d suggest that the good agreement between measurements and the predictions of reference 11 was a little fortuitous and due, probably, to the assumptions made in the region immediately downstream of the slot. Of course, the fact that the integration can be begun at the slot exit is a considerable practical advantage but it seems probable, in the light of the present measurements that a constant Schmidt (or Prandtl) number is an oversimplification and that a more realistic assumption will be required for the region immediately downstream of the slot exit.

The comparisons, so far, have been made with the author's own measurements for reasons which were stated earlier. Figure 10 presents two comparisons with data of other authors: these measurements were of the adiabatic wall effectiveness. The data of reference 14 included the initial profile and it may be seen that the resulting comparison is satisfactory if the linear Prandtl number distribution is assumed. On the other hand, the comparison with the effectiveness measurement of reference 13 is unsatisfactory: in this case, however, the initial temperature profile was not entirely compatible with the initial velocity profile.

The main implication of the comparisons presented in figures 8, 9 and 10 is that further work is necessary to establish the appropriate form of the effective Schmidt number.

5. Conclusions

i. The effect of an increase in the value of ρ_C/ρ_G is to increase the effectiveness, for a given value of $\bar{u}_C/u_G$: the quantitative effects are demonstrated by the measurements.

ii. For values of ρ_C/ρ_G above unity the optimum effectiveness is obtained with a value of $\bar{u}_C/u_G$ of approximately unity.

iii. For low values of ρ_C/ρ_G the optimum effectiveness is obtained with a value of $\bar{u}_C/u_G$ above unity.

iv. It is possible that the effectiveness obtained from a slot lip of constant thickness can be improved by tapering the lip to give a smaller thickness at the slot exit.

v. The prediction procedure prepared by S. V. Patankar, and D. B. Spalding can readily be applied to the film cooling situation in the region down stream of the immediate vicinity of the slot exit: the mixing length hypothesis leads to reasonable predictions of velocity profiles but further work is necessary to establish the appropriate effective Schmidt (or Prandtl) number distribution.

LIST OF SYMBOLS

Symbol	Meaning	Definition
c	mass fraction of injected fluid	
J	diffusional flux of injected fluid	
K	mixing length constant near the wall	
ℓ	mixing length	
m	mass flow ratio	$\frac{\rho_C \bar{u}_C}{\rho_G u_G}$
M	molecular weight	
p	static pressure	
R_c	slot Reynolds number	$\frac{\bar{u}_C y_C}{\nu_C}$
$\bar{R}$	universal gas constant	
s_S	local drag coefficient	$\frac{\tau_S}{\rho_G u_G^2}$
t	slot upper lip thickness	
T	absolute temperature	
u	velocity in x-direction	
$\bar{u}_C$	mean velocity at the slot	
u_G	velocity in the mainstream	
v	velocity in y-direction	
x	distance along the wall measured from the slot	
y	distance measured normal from the wall	
y_C	slot height	
y_G	velocity boundary-layer thickness	
ν	kinematic viscosity of fluid	
η_I	impervious-wall effectiveness	$\left(\equiv \frac{o_S - o_G}{o_C - o_G}\right)$
η	adiabatic-wall effectiveness	
ρ	fluid density	
μ_{eff}	effective viscosity	

Symbol	Meaning
μ	laminar viscosity
σ_{eff}	effective Prandtl or Schmidt number
τ	total (laminar + turbulent) shear stress
λ	mixing length constant in the outer region
ψ	stream function

Subscripts

C	pertaining the the flow through the slot
G	pertaining to the mainstream
S	pertaining to the wall

6. References

1. J. L. Stollery and A. A. M. El-Ehwany: On the use of a boundary-layer model for correlating film cooling data. Int. J. Heat Mass Transfer 10 (1967) 101.

2. R. J. Goldstein, R. B. Rask and E. R. G. Eckert: Film cooling with helium injection into an incompressible air flow. Int. J. Heat Mass Transfer 9 (1966) 1341.

3. R. J. Goldstein, E. R. G. Eckert, F. K. Tsou and A. Haji-Sheikh: Film cooling with air and helium injection through a rearward facing slot into a supersonic flow. A.I.A.A. Journal 4 (1966) 981.

4. S. S. Papell and A. M. Trout: Experimental investigation of air film cooling applied to an adiabatic wall by means of an axially discharging slot. N.A.S.A. TN D-9, (1959).

5. S. V. Patankar and D. B. Spalding: A finite difference procedure for solving the boundary-layer equations for two-dimensional flows. Int. J. Heat Mass Transfer. 10 (1967) 1389.

6. R. Shaw: The influence of hole dimensions on static pressure measurements. J. Fluid Mech. 7 (1960) 550.

7. J. H. Whitelaw: An experimental investigation of the two-dimensional wall jet. *Aero. Research Council* CP 942 (1967).

8. W. B. Nicoll and J. H. Whitelaw: The effectiveness of the uniform density, two-dimensional wall jet. Int. J. Heat Mass Transfer 10 (1967) 623.

9. J. H. Whitelaw: The effect of slot height on the effectiveness of the uniform density, two-dimensional wall jet. Imperial College, Department of Mechanical Engineering Report EHT/TN/4 (1967).

10. S. Sivasegaram and J. H. Whitelaw: Film cooling slots; the importance of lip thickness and injection angle. Imperial College, Department of Mechanical Engineering Report EHT/TN/6 (1967).

11. E. H. Cole, D. B. Spalding and J. L. Stollery: Film cooling effectiveness calculated by a finite-difference procedure. Imperial College, Department of Mechanical Engineering Report EHT/TN/3 (1967).

12. J. C. Rotta: Heat transfer and temperature distribution in turbulent boundary layers at supersonic and hypersonic flow. Agardograph 97, Part 1, (1965) 35.

13. R. A. Seban and L. H. Back: Velocity and temperature profiles in turbulent boundary layers with tangential injection. ASME, Journal of Heat Transfer, February 1962, 45.

14. J. P. Hartnett, R. C. Birkebak, E. R. G. Eckert: Velocity distributions, temperature distributions, effectiveness and heat transfer in a cooling of a surface with a pressure gradient. A.S.M.E., International Developments in Heat Transfer, Part IV (1961), 682.

Table 1

Impervious wall effectiveness: Hydrogen injection

Density ratio = 0.069

Slot height = 0.100 in.

	Run 1	Run 2	Run 3	Run 4	Run 5	Run 6
$\bar{u}_C/u_G$	0.308	0.560	0.775	1.05	1.27	1.52
m	0.021	0.0388	0.054	0.073	0.088	0.105
R_C	70.8	129.0	173.0	233.0	282.0	340.0
x/y_C						
2.5	0.612	0.872	0.774	1.00	0.870	0.655
12.5	0.0403	0.1310	0.1795	0.2640	0.2640	0.3160
32.5	0.0186	0.0295	0.0505	0.0825	0.0855	0.1208
52.5	0.0130	0.0229	0.0328	0.0462	0.0612	0.0778
72.5	0.0097	0.0169	0.0256	0.0374	0.0458	0.0640
92.5	0.0085	0.0147	0.0214	0.0268	0.0344	0.0480
112.5	0.0079	0.0119	0.0178	0.0255	0.0304	0.0417
132.5	0.0071	0.0115	0.0168	0.0209	0.0256	0.0352
172.5	0.0057	0.0092	0.0130	0.0181	0.0206	0.0270
212.5	0.0052	0.0081	0.0111	0.0160	0.0177	0.0230

Table 2

Impervious wall effectiveness: Air injection

Density ratio = 1.0

Slot height = 0.100 in.

	Run 6	Run 5	Run 4	Run 7	Run 1	Run 8	Run 2	Run 3
m	0.37	0.575	0.763	1.035	1.23	1.74	2.16	3.12
R_C	1285	1990	2620	3540	4170	5700	7150	10510
x/y_C								
2.5	0.806	0.725	0.879	0.770	0.920	0.920	0.929	1.00
12.5	0.842	0.930	0.966	0.955	0.965	0.994	0.950	1.00
32.5	0.418	0.655	0.770	0.800	0.825	0.818	0.815	0.805
52.5	0.244	-	-	0.661	-	0.694	-	0.680
72.5	0.205	0.405	0.587	0.635	0.610	0.636	0.594	0.587
92.5	0.167	0.318	0.510	0.565	0.605	0.587	0.493	0.525
112.5	0.150	0.288	0.455	0.540	0.562	0.555	0.521	0.473
132.5	0.128	0.244	0.384	0.511	0.530	0.476	0.479	0.442
172.5	0.108	0.210	0.303	0.461	0.416	0.456	0.394	0.370
212.5	0.092	0.170	0.282	0.394	0.394	0.412	0.398	0.366

Table 3

Impervious wall effectiveness: Argon injection

Density ratio = 1.38

Slot height = 0.100 in.

	Run 1	Run 2	Run 3	Run 4	Run 5	Run 8	Run 7	Run 6
$\bar{u}_C/u_G$	0.292	0.458	0.600	0.825	0.982	1.340	1.710	2.480
m	0.403	0.632	0.830	1.140	1.357	1.850	2.36	3.42
R_C	1065	1670	2180	2980	3550	4800	6050	8720
x/y_C								
2.5	0.935	0.910	0.910	0.935	0.950	0.919	0.986	0.999
12.5	0.785	0.905	0.951	0.991	0.975	0.935	0.989	0.998
32.5	0.478	0.688	0.785	0.865	0.866	0.830	0.918	0.877
52.5	0.331	0.510	0.628	0.810	0.775	0.730	0.745	0.756
72.5	0.273	0.396	0.545	0.720	0.720	0.685	0.690	0.690
92.5	0.245	0.329	0.478	0.667	0.690	0.660	0.638	0.639
112.5	0.218	0.288	0.457	0.620	0.660	0.633	0.617	0.616
132.5	0.194	0.254	0.368	0.580	0.620	0.607	0.570	0.575
172.5	0.171	0.207	0.332	0.498	0.562	0.558	0.529	0.525
212.5	0.153	0.175	0.266	0.446	0.500	0.532	0.480	0.482

Table 4

Impervious wall effectiveness: Arcton 12 injection

Density ratio = 4.17

Slot height = 0.100 in.

	Run 7	Run 1	Run 2	Run 3	Run 4	Run 5	Run 6
$\bar{u}_C/u_G$	0.281	0.435	0.575	0.782	0.884	1.26	1.645
m	1.17	1.815	2.40	3.26	3.68	5.25	6.87
R_C	2450	3900	5150	7000	8140	11000	14250
x/y_C							
2.5	0.985	0.998	1.00	0.998	0.995	1.00	0.996
12.5	0.915	0.979	0.995	0.997	1.000	1.00	0.996
32.5	0.630	0.880	0.945	0.973	0.975	0.985	0.990
52.5	0.473	0.780	0.886	0.930	0.936	0.960	0.960
72.5	0.382	0.646	0.828	0.910	0.920	0.940	0.940
92.5	0.316	0.630	0.722	0.885	0.885	0.925	0.922
112.5	0.304	0.568	0.761	0.857	0.870	0.908	0.905
132.5	0.278	0.512	0.635	0.815	0.840	0.897	0.890
172.5	0.224	0.442	0.613	0.802	0.785	0.870	0.870
212.5	0.197	0.394	0.540	0.745	0.752	0.835	0.845

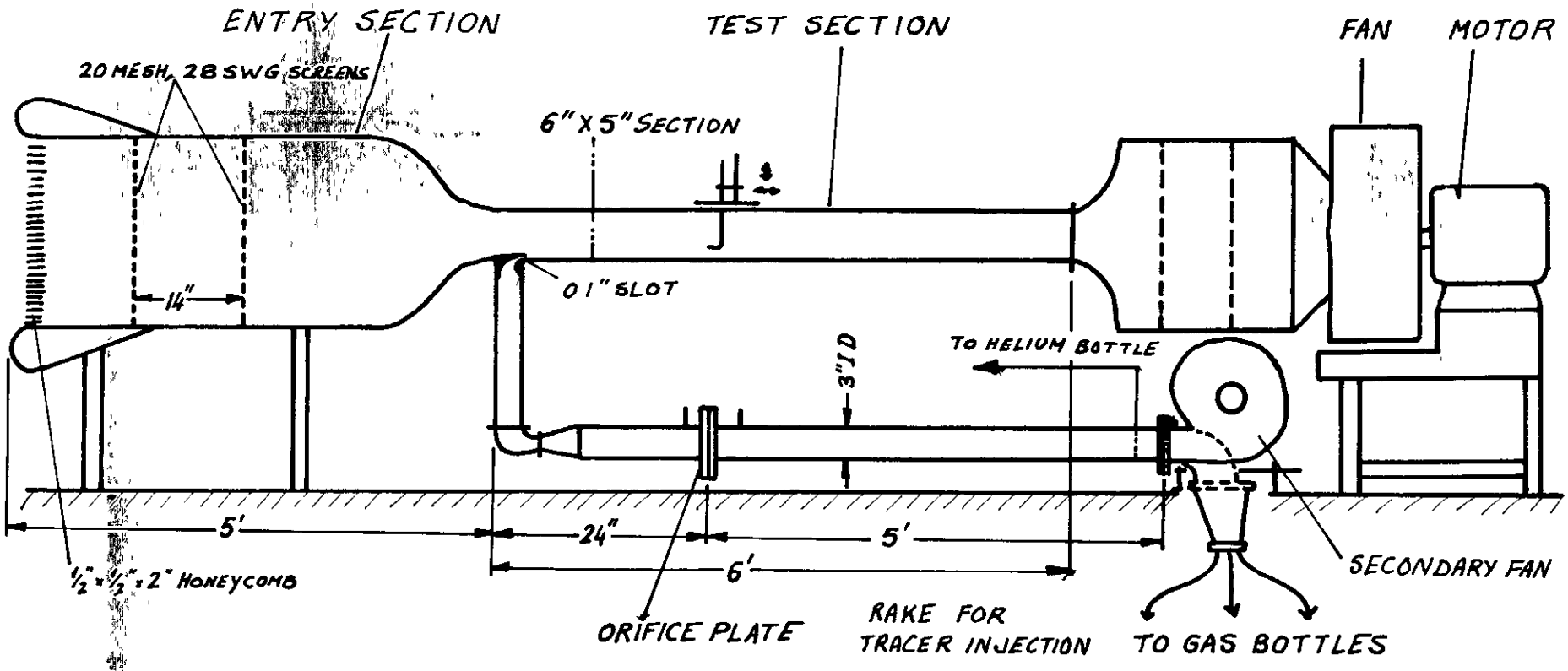

FIG 1 SCHEMATIC DIAGRAM OF WIND TUNNEL

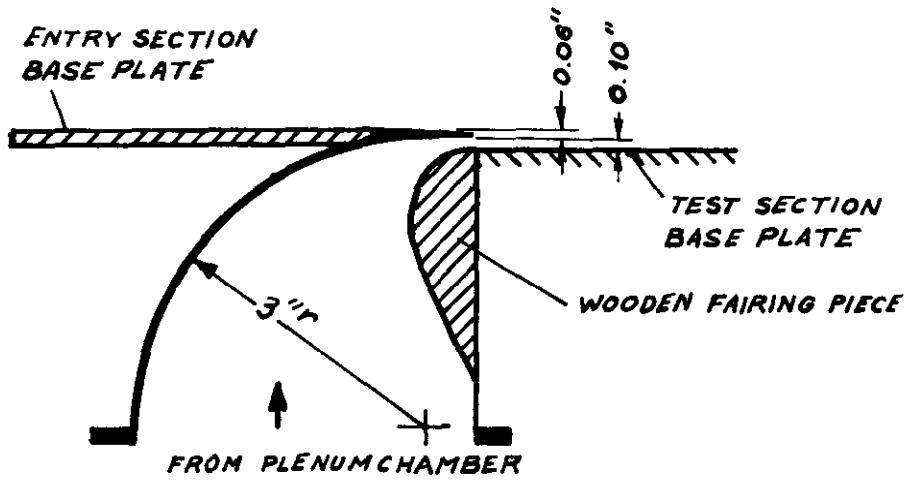

FIG 2. THE INJECTION SLOT

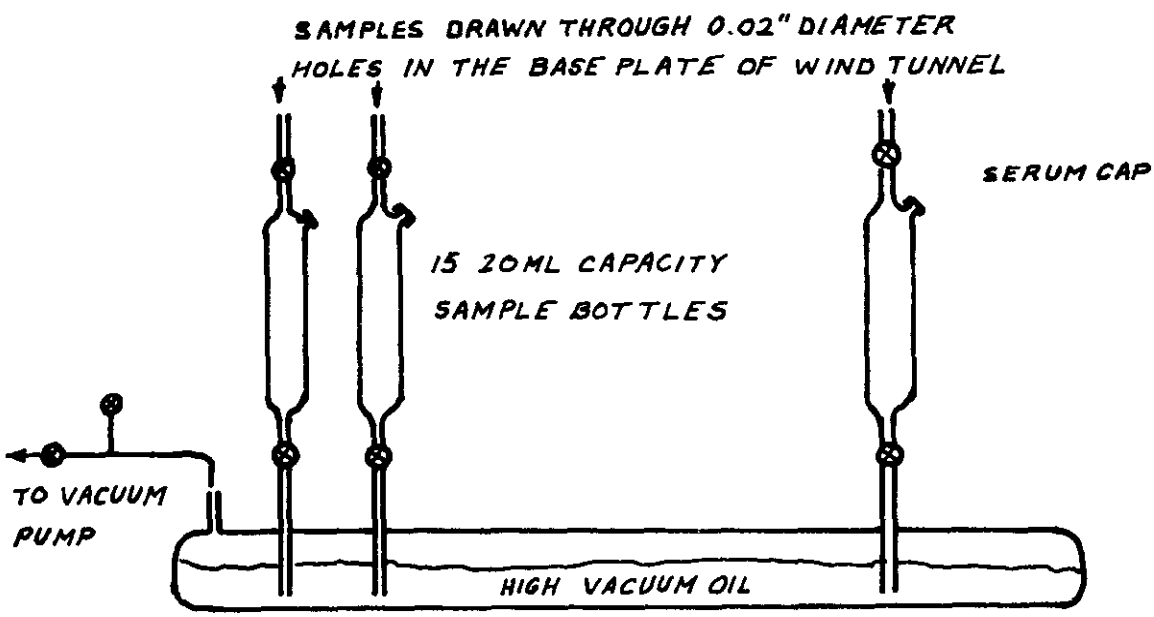

FIG. 3 SAMPLING SYSTEM

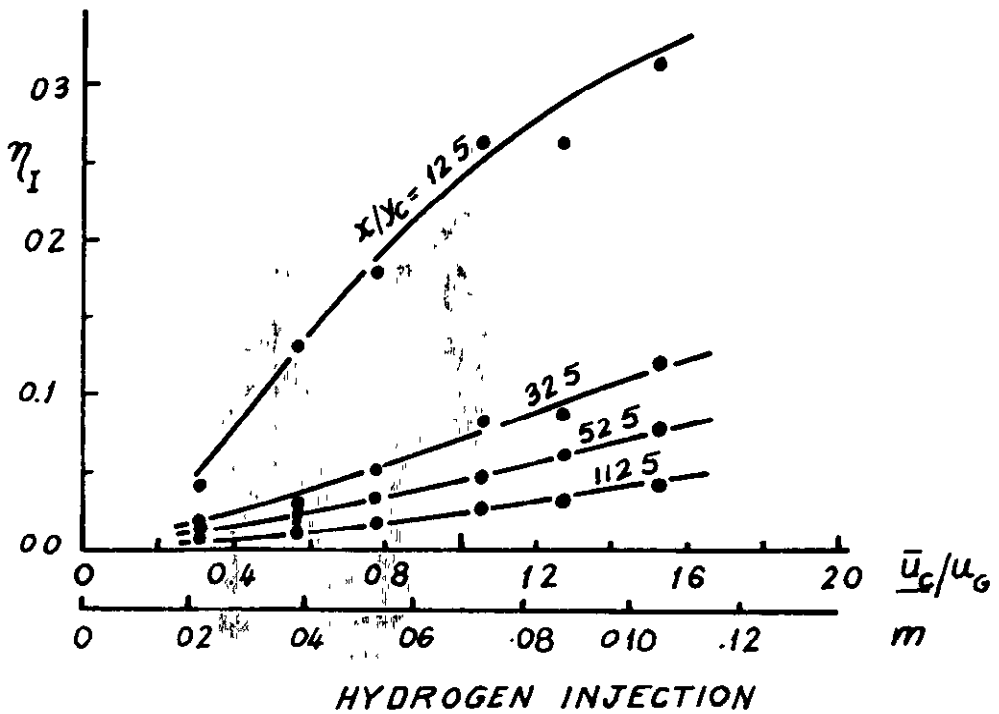

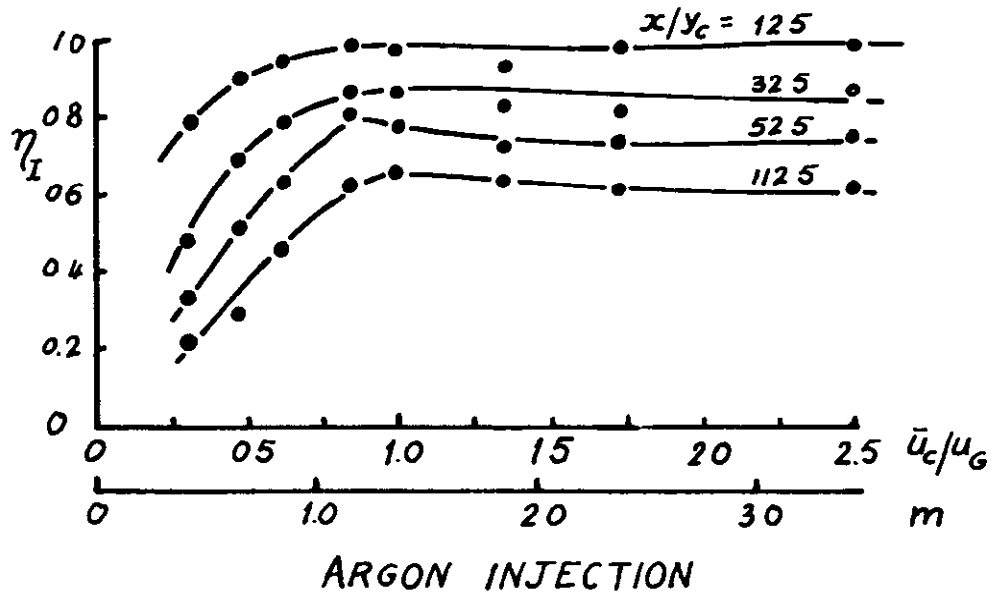

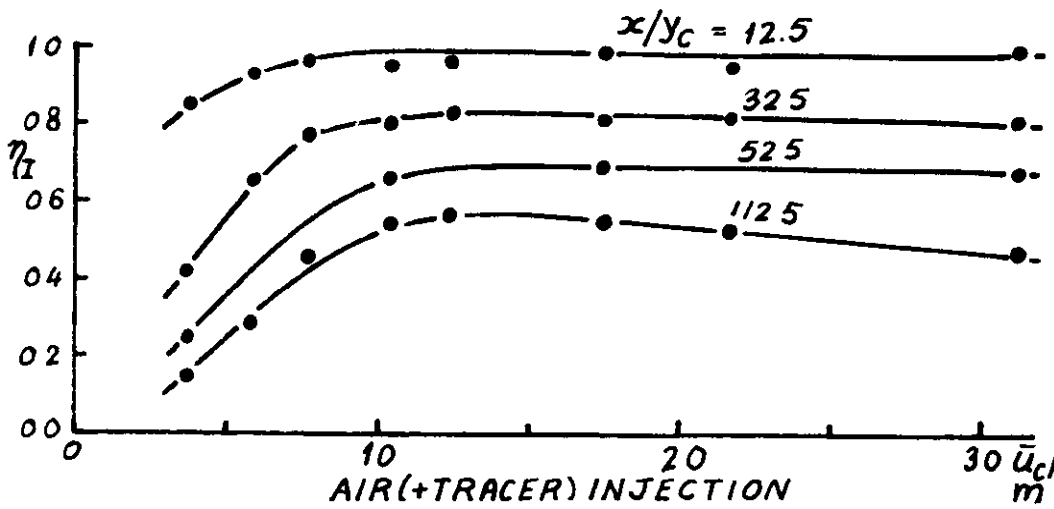

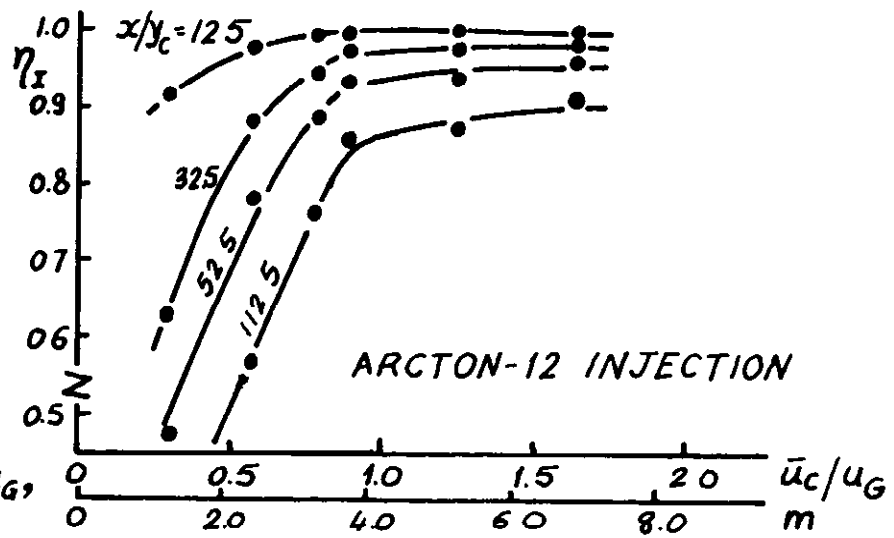

FIG 4. MEASURED VALUES OF IMPERVIOUS WALL EFFECTIVENESS – η_I AGAINST $\bar{u}_c/u_G$

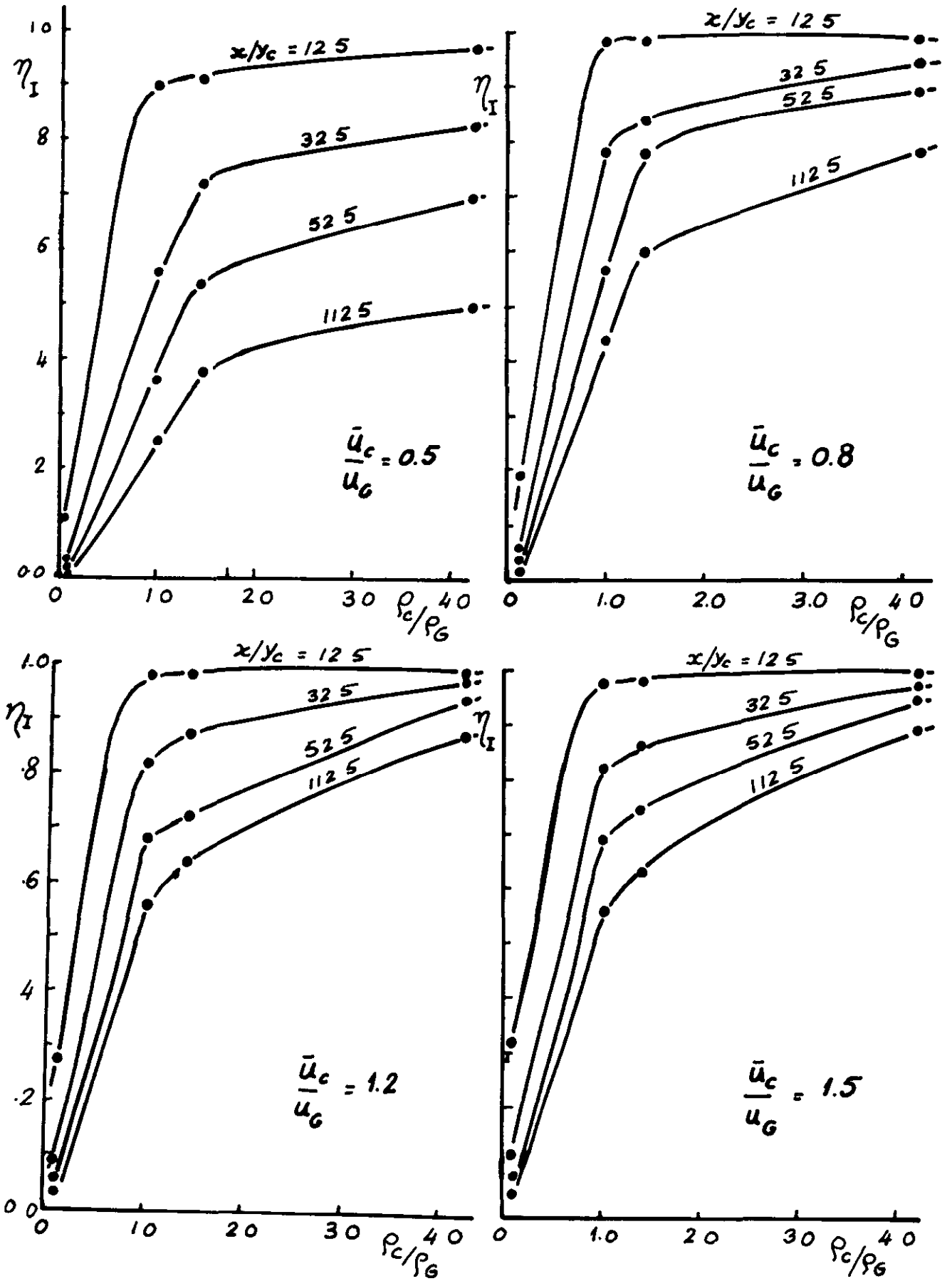

FIG.5 MEASURED VALUES OF THE IMPERVIOUS WALL EFFECTIVENESS. η_I AGAINST ρ_c/ρ_G

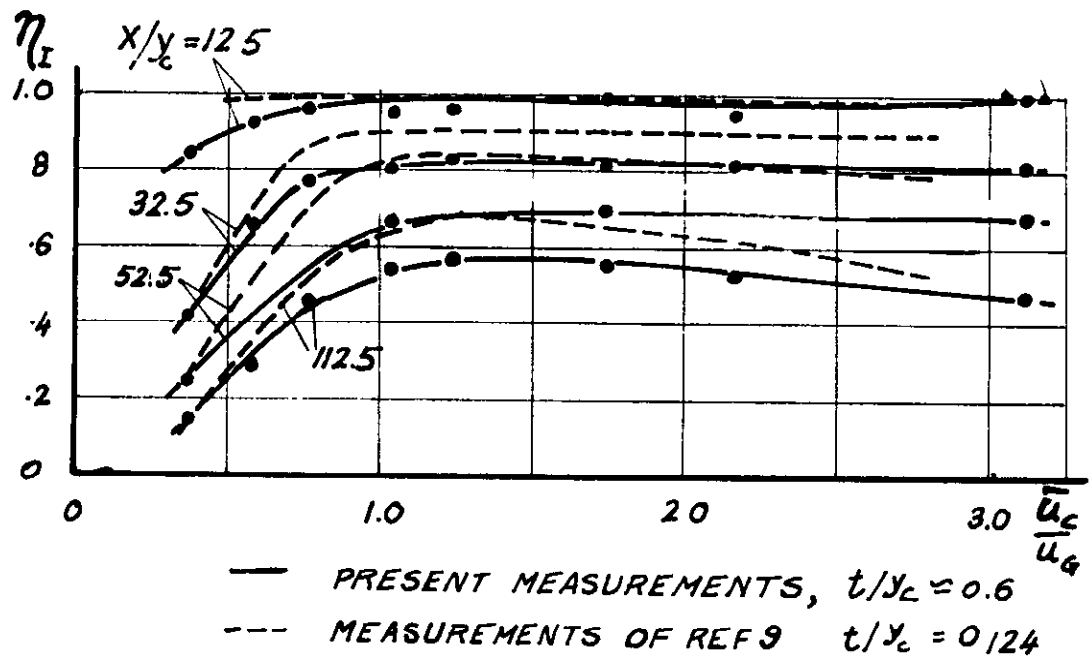

FIG 6 COMPARISON OF PRESENT AIR INJECTION MEASUREMENTS WITH THOSE OF REFERENCE 9

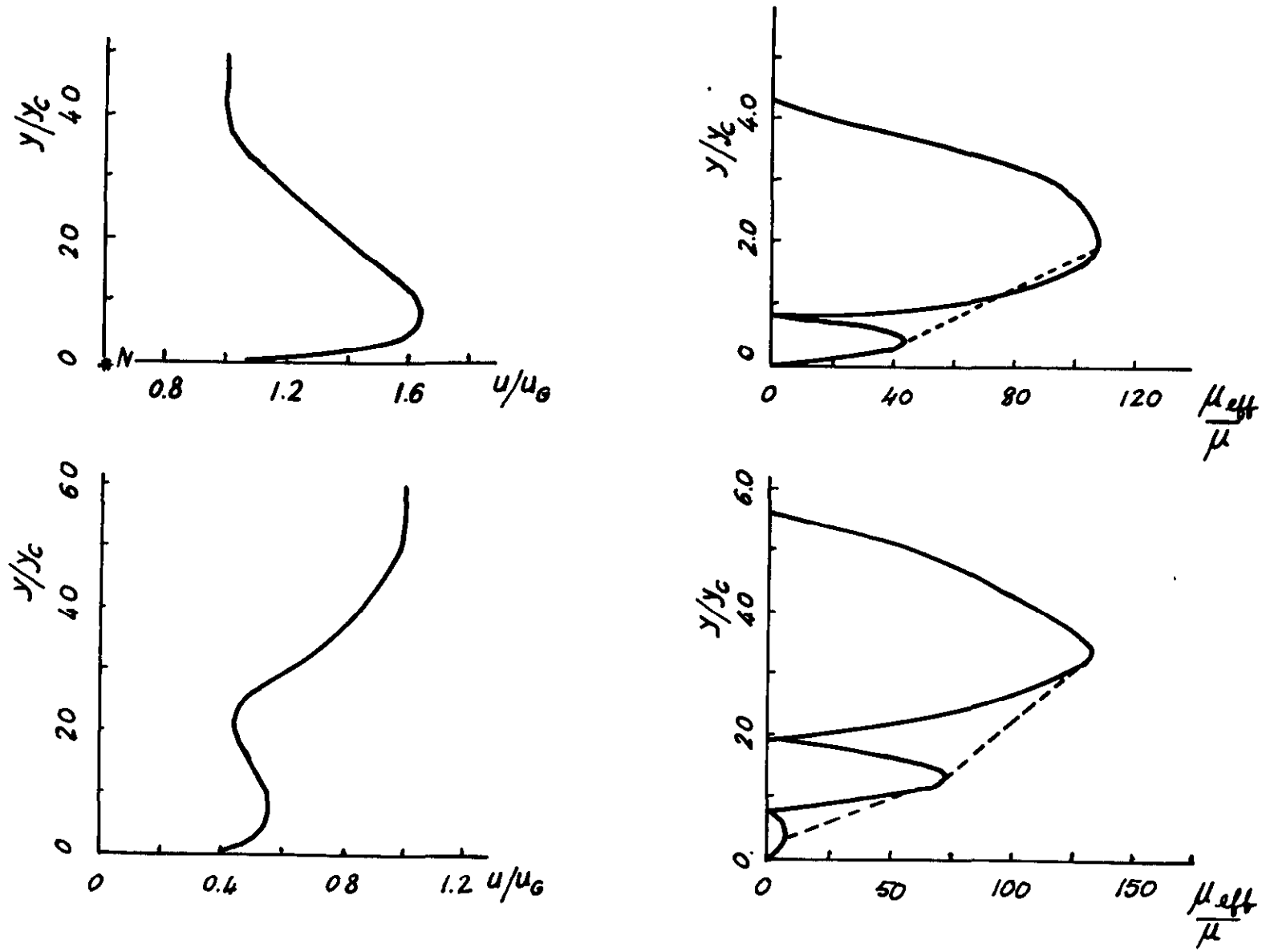

FIG 7 EDDY VISCOSITY PROFILES RESULTING FROM A RAMP MIXING-LENGTH DISTRIBUTION

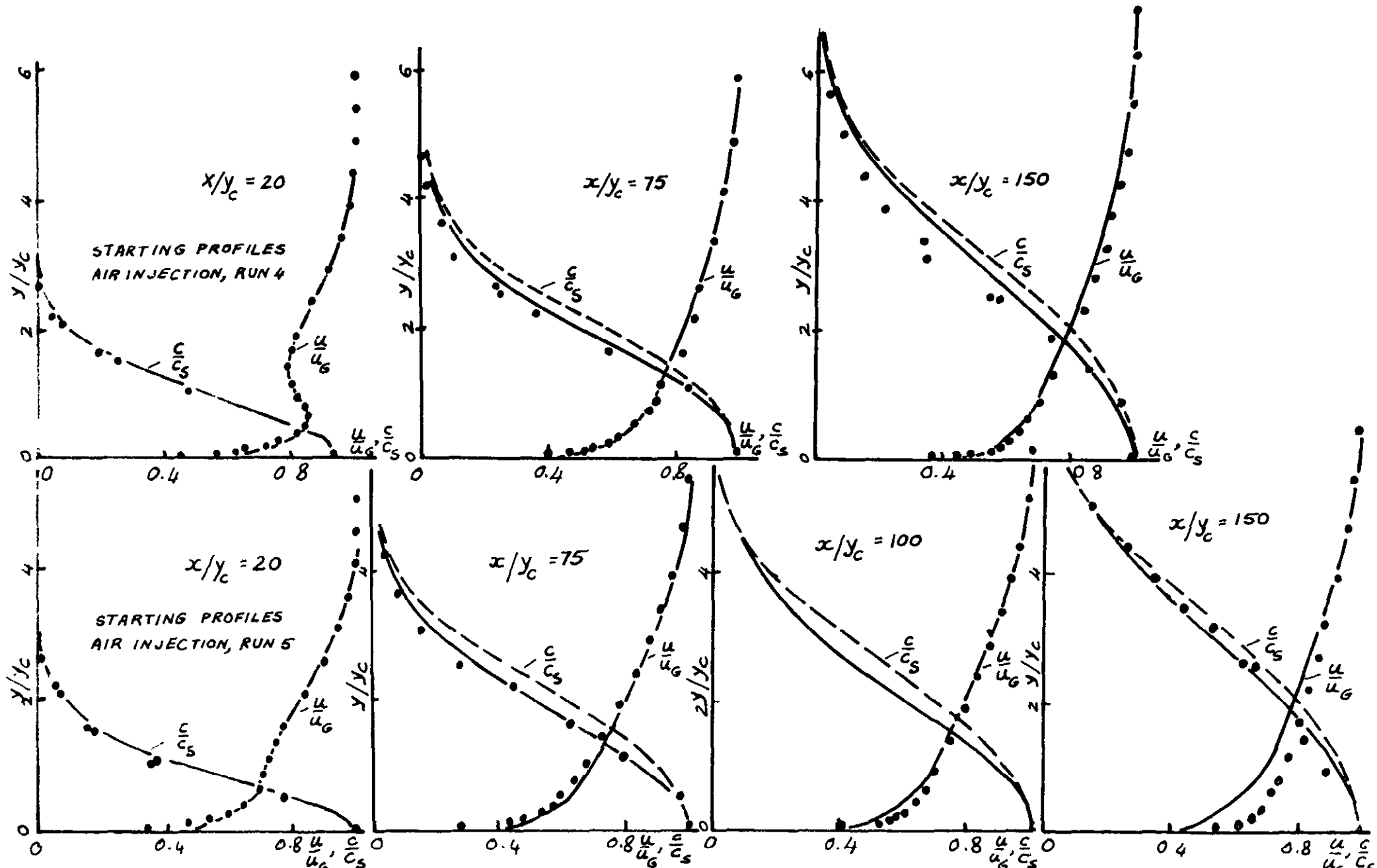

FIG.8. COMPARISON BETWEEN EXPERIMENTAL AND PREDICTED PROFILES

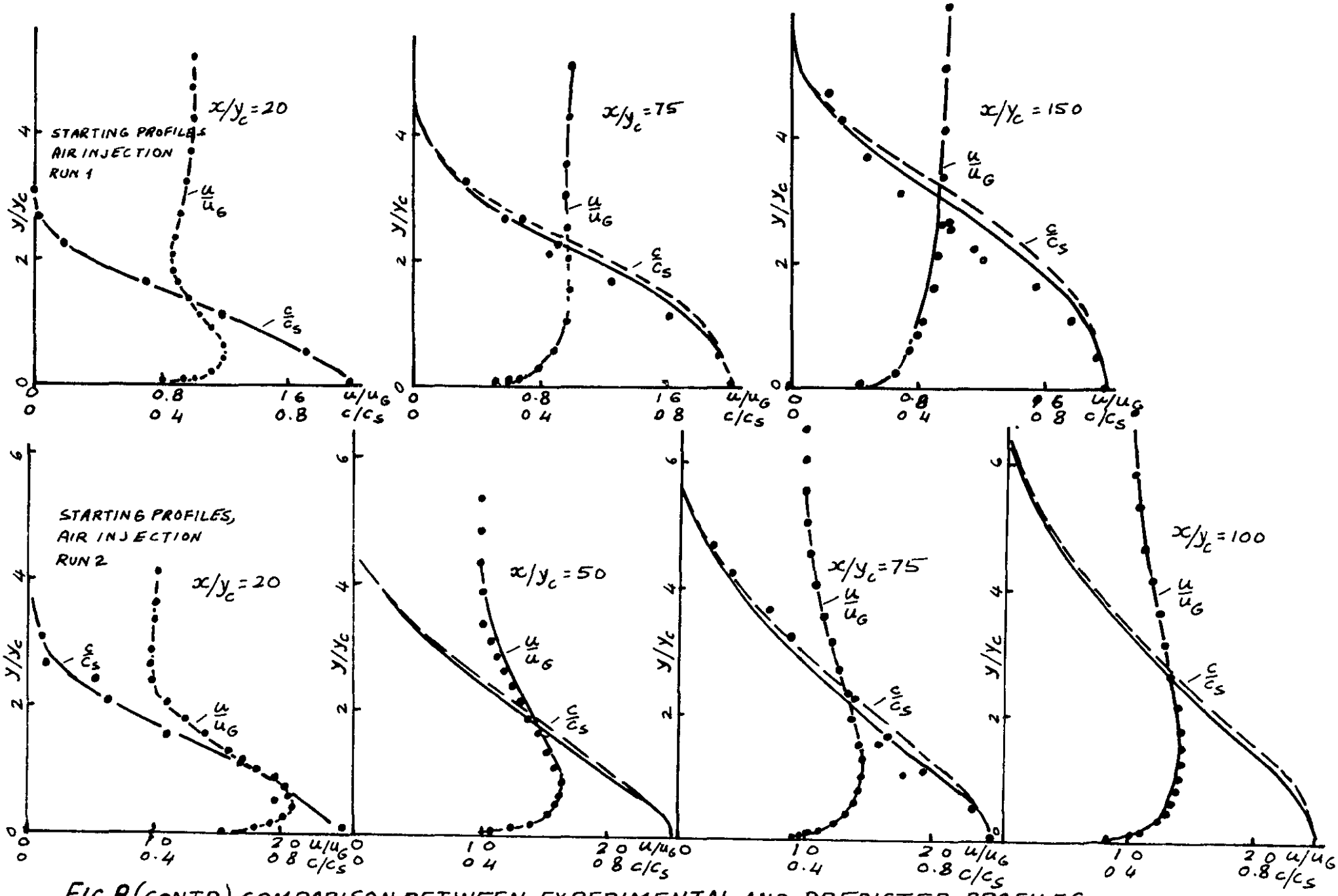

FIG. 8 (CONTD) COMPARISON BETWEEN EXPERIMENTAL AND PREDICTED PROFILES

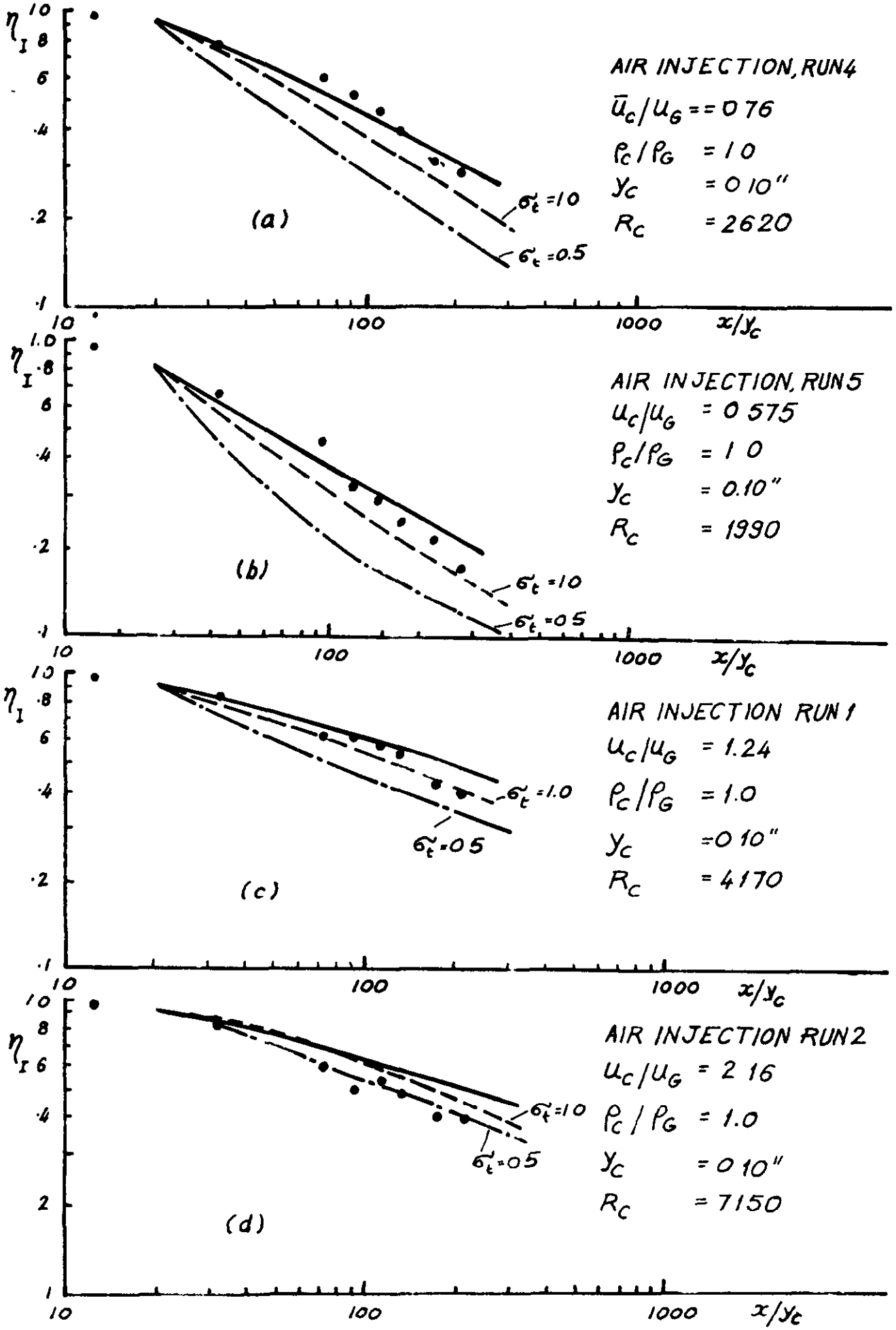

FIG 9 COMPARISON OF EXPERIMENTAL AND PREDICTED VALUES OF EFFECTIVENESS · PRESENT MEASUREMENTS

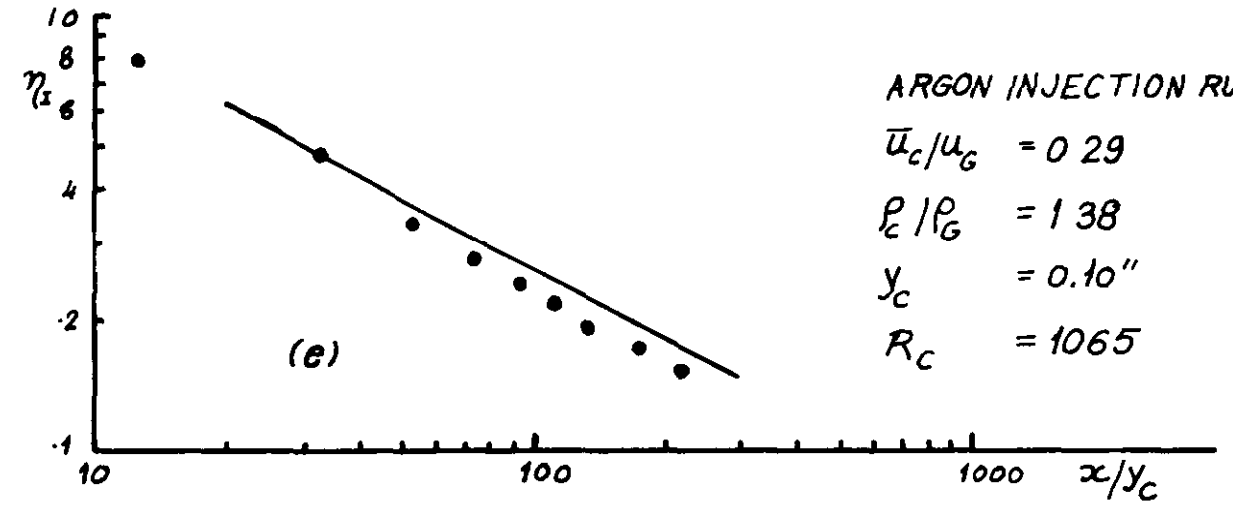

ARGON INJECTION RUN 1

$\bar{u}_c/u_G$ = 0 29

ρ_c/ρ_G = 1 38

y_c = 0.10"

R_c = 1065

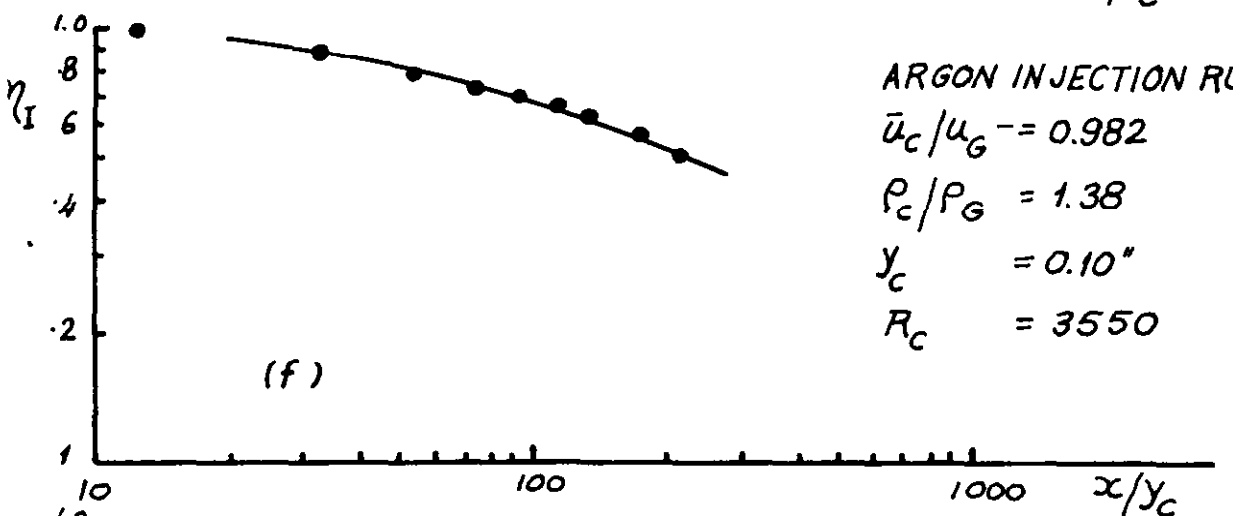

ARGON INJECTION RUN 5

$\bar{u}_c/u_G$ = 0.982

ρ_c/ρ_G = 1.38

y_c = 0.10"

R_c = 3550

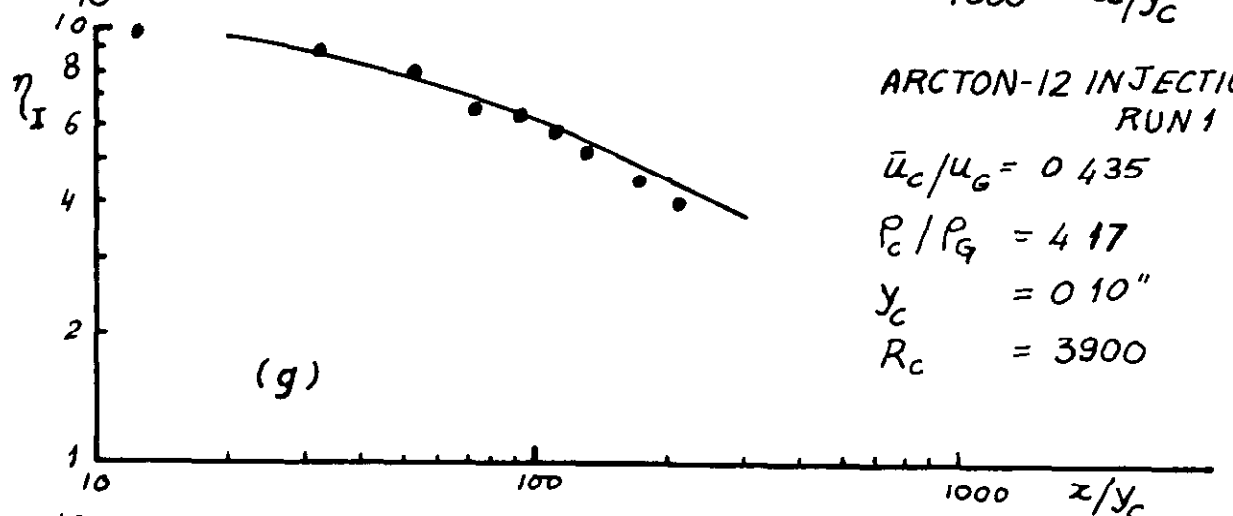

ARCTON-12 INJECTION, RUN 1

$\bar{u}_c/u_G$ = 0 435

ρ_c/ρ_G = 4 17

y_c = 0 10"

R_c = 3900

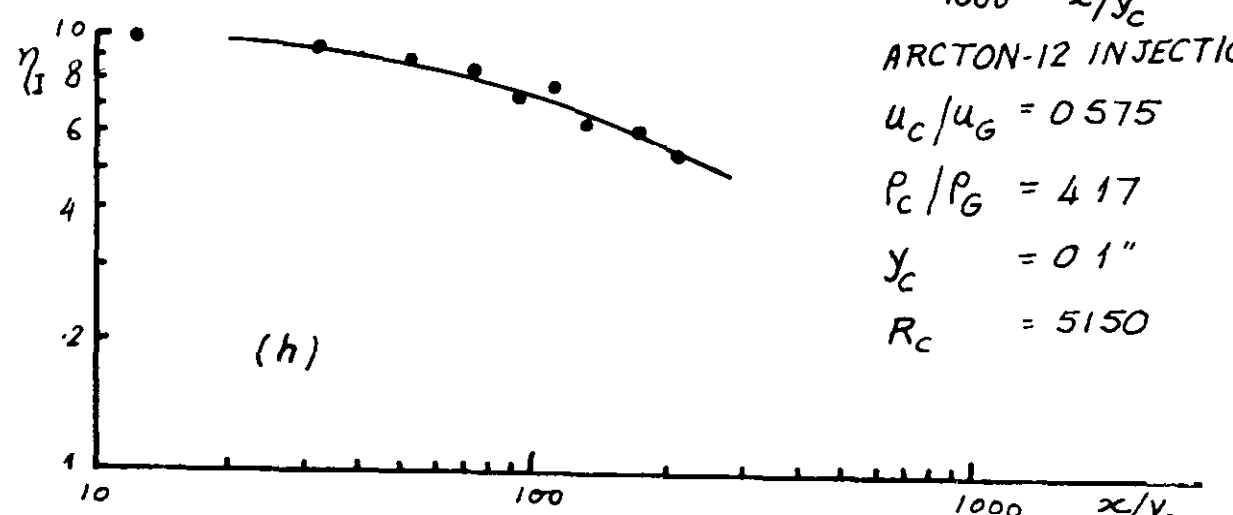

ARCTON-12 INJECTION

u_c/u_G = 0 575

ρ_c/ρ_G = 4 17

y_c = 0 1"

R_c = 5150

FIG 9 (CONTD) COMPARISON OF EXPERIMENTAL AND PREDICTED VALUES OF EFFECTIVENESS PRESENT MEASUREMENTS

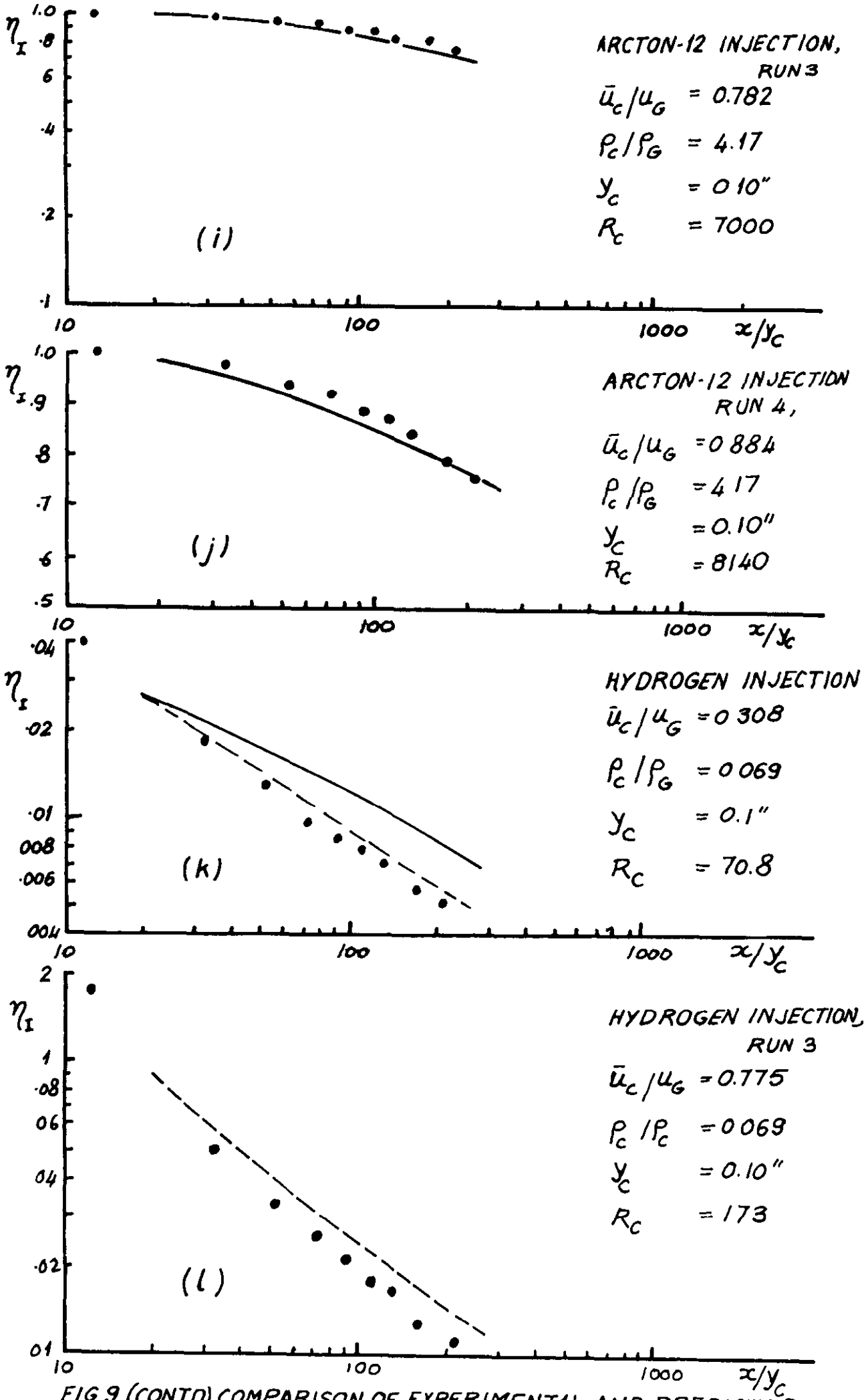

FIG 9 (CONTD) COMPARISON OF EXPERIMENTAL AND PREDICTED VALUES OF EFFECTIVENESS : PRESENT MEASUREMENTS

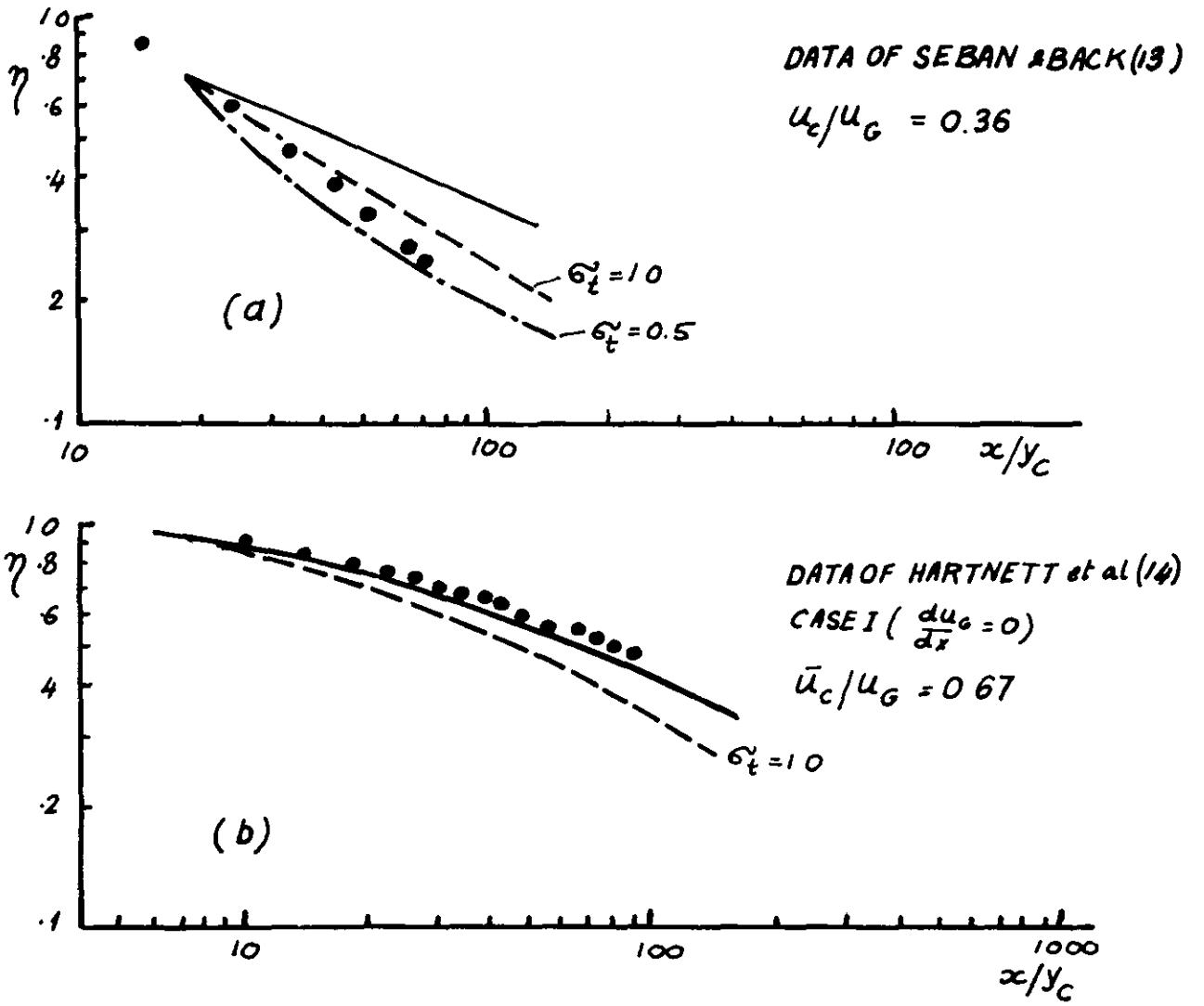

FIG 10 COMPARISON OF EXPERIMENTAL AND PREDICTED VALUES OF EFFECTIVENESS · DATA OF REFS (13) AND (14).

A.R.C. C.P. No.1013
December 1967

Pai, B.R. and Whitelaw, J. H.

THE INFLUENCE OF DENSITY GRADIENTS ON THE EFFECTIVENESS OF FILM COOLING

New measurements of the impervious-wall effectiveness are presented in the range of the velocity ratio $0.3 \leq \bar{u}_C/u_G \leq 3.1$.

These measurements were carried out using hydrogen, air, argon and Arcton 12 as the injected gas: the resulting range of density ratios was $0.07 \leq \rho_C/\rho_G \leq 4.17$.

(over)

A.R.C. C.P. No.1013
December 1967

Pai, B.R. and Whitelaw, J.H.

THE INFLUENCE OF DENSITY GRADIENTS ON THE EFFECTIVENESS OF FILM COOLING

New measurements of the impervious-wall effectiveness are presented in the range of the velocity ratio $0.3 \leq \bar{u}_C/u_G \leq 3.1$.

These measurements were carried out using hydrogen, air, argon and Arcton 12 as the injected gas: the resulting range of density ratios was $0.07 \leq \rho_C/\rho_G \leq 4.17$.

(over)

A.R.C. C.P. No.1013
December 1967

Pai, B.R. and Whitelaw, J.H.

THE INFLUENCE OF DENSITY GRADIENTS ON THE EFFECTIVENESS OF FILM COOLING

New measurements of the impervious-wall effectiveness are presented in the range of the velocity ratio $0.3 \leq \bar{u}_C/u_G \leq 3.1$.

These measurements were carried out using hydrogen, air, argon and Arcton 12 as the injected gas: the resulting range of density ratios was $0.07 \leq \rho_C/\rho_G \leq 4.17$.

(over)

The measurements demonstrate, quantitatively, that an increase in the density ratio leads to an increase in effectiveness for the same velocity ratio.

The prediction method proposed by S. V. Patankar and D. B. Spalding has been tested against the present measurements and shown to be a convenient method in the region downstream of the immediate vicinity of the slot exit. The predictions are reasonable but it is concluded that further experimental work is necessary to establish the appropriate distribution of the effective Schmidt (or Prandtl) number.

The measurements demonstrate, quantitatively, that an increase in the density ratio leads to an increase in effectiveness for the same velocity ratio.

The prediction method proposed by S. V. Patankar and D. B. Spalding has been tested against the present measurements and shown to be a convenient method in the region downstream of the immediate vicinity of the slot exit. The predictions are reasonable but it is condluded that further experimental work is necessary to establish the appropriate distribution of the effective Schmidt (or Prandtl) number.

The measurements demonstrate, quantitatively, that an increase in the density ratio leads to an increase in effectiveness for the same velocity ratio.

The prediction method proposed by S. V. Patankar and D. B. Spalding has been tested against the present measurements and shown to be a convenient method in the region downstream of the immediate vicinity of the slot exit. The predictions are resonable but it is concluded that further experimental work is necessary to establish the appropriate distribution of the effective Schmidt (or Prandtl) number.

D 106847/1/135645 K.3 9/68 P

Printed and published by
HER MAJESTY'S STATIONERY OFFICE

To be purchased from
49 High Holborn, London W.C 1
13A Castle Street, Edinburgh 2
109 St. Mary Street, Cardiff CF1 1JW
Brazennose Street, Manchester M60 8AS
50 Fairfax Street, Bristol BS1 3DE
258 Broad Street, Birmingham 1
7 Linenhall Street, Belfast BT2 8AY
or through any bookseller

Printed in England

SO Code No 23-9018-13